parameters are $E_0 = 8.427$ Mev, $\Gamma_0 = 15$ kev. Again, we see that the background cross section is significantly different from the hard sphere or optical potential cross sections. Also the energy dependent hard sphere radius needed to fit the background cross section shows qualitatively the same behavior as in model A.

The parameters have been chosen in both cases, so that the energy of the resonance when the coupling goes to zero, $\bar{E}$, is the same. This energy is that of the nearest level in the uncoupled infinite square well representing the compound nucleus mode of motion. For these parameters, this energy is 5.904 Mev. (The compound nucleus well in model B has twice the radius as the compound nucleus well in model A so that the level density is twice as great, but the levels in such a well are separated by energies of the order of 20 Mev at this energy. Therefore, the separation of resonances in the scattering cross section is large compared to the widths of the resonances when the coupling is weak. Thus we are dealing with well isolated resonances in both cases.) The strength of the coupling in both models has been adjusted so that the total widths of the resonances, Γ_0, is small, and so that Γ_0 is approximately the same for the two resonances. In this case,

the reduced widths $\gamma^2 = \Gamma/2kR_1$ in both models will be roughly the same if the resonance energies are the same. This means that the probability of forming the compound mode of motion in both cases is essentially the same. Using this effect as a measure of the coupling, we can then say the strengths of the coupling in the two cases are roughly the same.

There are two points that can be made. One is that in general the shape of the resonance is not strongly model dependent, while the level shift and the background cross section are quite sensitive to the details of the coupling mechanism. The second point arises from the realization that the widths of the resonances shown in Figs. 1 and 3 are small in comparison with experimentally observed widths. The reduced widths are 4 and 2 kev for models A and B, respectively. Thus the coupling is weak. However, the shifts in the resonance energies from $\bar{E}$, the Δ's, are large ($\Delta \cong -3.3$ Mev in model A, $\Delta \cong +2.5$ Mev in model B). Also, even though the resonances are well isolated for these cases and the coupling is weak, the background cross section differs significantly from the zero-coupling cross section. Therefore it is evident that even in the weak-coupling limit, sizable effects can occur.

Fluorescent Response of Scintillation Crystals to Heavy Ions*

E. Newman, A. M. Smith, and F. E. Steigert
Yale University, New Haven, Connecticut
(Received January 27, 1961)

The light output of CsI(Tl) was measured as a function of energy for incident ions of B^{10}, B^{11}, C^{12}, N^{14}, O^{16}, and F^{19}. The response of NE 102 plastic and anthracene scintillators was also measured for ions of N^{14} and O^{16}, respectively. The response of CsI was essentially linear for energies above 6 Mev/A, where A is the mass number of the incident ion. The NE 102 was linear for energies above 4 Mev/A. The anthracene data showed slight curvature even at 9 Mev/A. It would appear that the response of CsI differs somewhat among crystal samples.

INTRODUCTION

DURING the search for suitable particle detectors for heavy ions, a systematic survey of various scintillation crystals was undertaken by various groups at this laboratory. As has already been reported,[1,2] the alkali halides proved generally superior in performance because of their higher light output and correspondingly better resolution. The CsI(Tl) crystals demonstrated one rather strange characteristic, however. There appeared to be a reproducible difference in luminescence among crystals obtained at different times from different

sources. This variation could be reliably associated with the pulse height ratio between the ThC and ThC' alpha particle groups. The organic and plastic scintillators used, as well as having a total light output somewhat lower than that of the CsI, showed rather significant differences in general behavior. Hopefully, in these variations lies the clue to a better understanding of the mechanisms involved in the scintillation process.

EXPERIMENTAL RESULTS

The experimental data were obtained in the manner previously described.[1] Particle beams from the Yale heavy-ion linear accelerator were magnetically analyzed, degraded with nickel absorbing foils, and then re-analyzed in a magnet spectrometer. The detection system consisted of $\frac{1}{2}$-in. diameter by $\frac{1}{2}$- to 1-mm thick crystals

[1] E. Newman and F. E. Steigert, Phys. Rev. 118, 1575 (1960); see also, Bull. Am. Phys. Soc. 4, 51 (1959); 4, 270 (1959).
[2] A. R. Quinton, C. E. Anderson, and W. J. Knox, Phys. Rev. 115, 886 (1959).

mounted directly onto the face of a DuMont 6292 photomultiplier. The analyzed particles were restricted to the central portion of the detector by means of a $\frac{1}{4}$-in. diam collimator. The pulse-height spectrum was observed on an Atomic 20-channel analyzer. Various phototube voltages from 800–1200 v were used to insure that there were no space charge limitations. The relative pulse heights obtained are displayed in Figs. 1–3. In each case, the normalization is in terms of the pulse height of the ThC' alpha particle (8.78 Mev) taken as unity.

In Fig. 1 are displayed the data as obtained for the various ion species in CsI. A is the mass number of the incident ion. The curves for the two boron isotopes and fluorine are explicitly drawn for the entire range of observed energy values. Experimental points are shown only for the fluorine to avoid unnecessary confusion. As is evident, all of the curves have the same approximate shape and converge for low velocities. The curves for C^{12} and O^{16} are arbitrarily terminated at about 4.5 Mev/A to avoid confusion in the general low-energy convergence. The nitrogen curve is experimentally indistinguishable from that of the B^{11}, when plotted in the fashion shown. All of the curves appear to be linear above 6 Mev/nucleon. For all of the scintillators tested, the resolution varied inversely as the square root of the energy. Typical values for full-energy ions in CsI were of the order of 2%.

A comparison of these data with the results obtained in contemporary experiments by Quinton et al.[2] displayed a marked discrepancy. In general, the corresponding curves of reference 2 demonstrated a systematic displacement to lower relative pulse heights.

This effect could be best labeled in terms of the pulse height ratios obtained between the ThC and ThC' alpha particles of 6.05 and 8.78 Mev, respectively. The crystal blanks used in the present experiment consistently yielded a value of 0.60, significantly below the ratio of 0.64 typical of reference 2. Such a lower ratio could well be accounted for in terms of a relatively insensitive surface layer equivalent to about 0.45 mg/cm^2 of absorber. Unfortunately, adjustment of the heavy-ion data commensurate with such an assumption did not materially alter the nature of the discrepancies. Two attempts were made to resolve the apparent disagreement experimentally. First, a crystal blank borrowed from Quinton et al. was used in our apparatus. As was to be expected, the data reproduced their results. Finally, the surfaces of the crystals used in the present experiment were repeatedly polished down in an attempt to remove the hypothesized dead layer. Again, the results were unchanged. The inescapable conclusion would thus appear to be that a degree of variation exists among some CsI crystals. Such nonreproducibility has been observed elsewhere as well.[3]

While the source of these differences is not yet understood, two possible mechanisms are being considered. Differences in the thallium concentration might be expected to give results of this type. It is also conceivable that such deviations might result from the existence of preferential axes for luminescence within the crystal lattice.[4] Such an effect might be more pronounced in CsI than in NaI, considering the difference in crystal structure. Further, since the former usually exist as sawed rather than cleaved blanks, a somewhat random orientation of crystalline axes might be expected in any given stock of scintillators. This possibility is presently being investigated.

The data for the anthracene are displayed in Fig. 2. The general characteristics would appear to be quite similar to those exhibited by the alkali halides: a
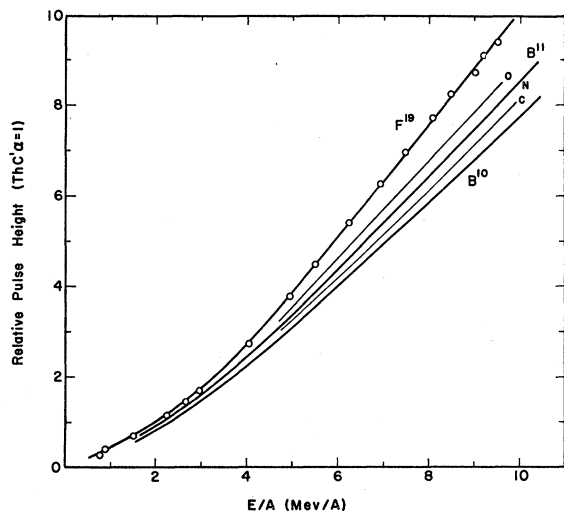

FIG. 1. Light output of CsI(Tl) crystals as a function of energy per nucleon for ions of boron, carbon, nitrogen, oxygen, and fluorine. Vertical scale is normalized relative to 8.78 Mev alpha particles from ThC'. The N^{14} and B^{11} are experimentally indistinguishable. The C^{12} and O^{16} curves are arbitrarily cut off at about 4.5 Mev/A to prevent confusion in the general low-energy convergence.
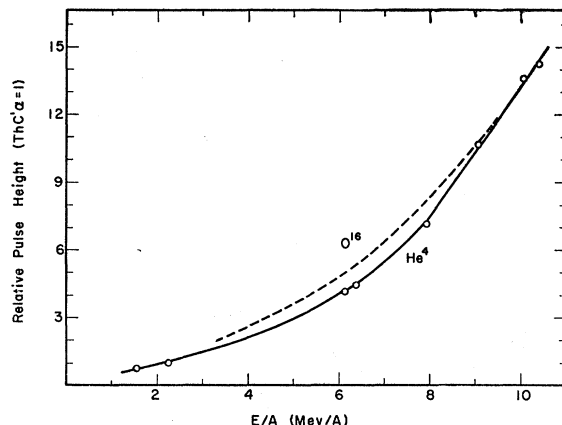
[3] M. L. Halbert (private communication).
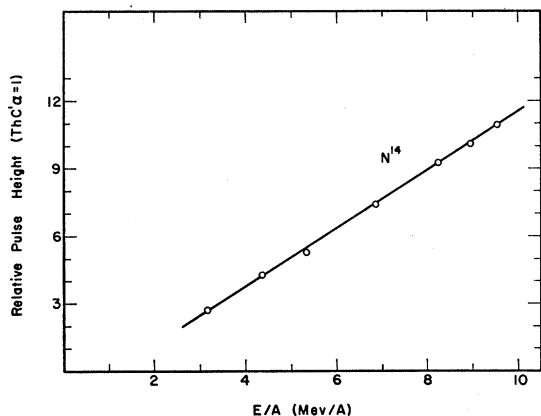[4] R. G. Wheeler (private communication).

FIG. 3. Light output of NE 102 plastic scintillator as a function of energy per nucleon for nitrogen ions.

gradual increase in luminous efficiency with velocity and becoming linear somewhere in the neighborhood of 9 Mev/nucleon. However, this type of behavior is quite antipodal to that observed by Taylor et al.[5] for alpha particles. In this latter work, the total light output as a function of energy shows a negative curvature and appears to be saturating at about 2 Mev/ nucleon. Even though an effective surface absorption could not precipitate such an inversion, the same checks as with the CsI were performed. Again, the ThC-ThC' alpha-particle pulse-height ratio (0.74 in this case) did not change with repeated polishing. This invariance would also seem to rule out any nonlinear sensitivity gradients. It should be noted that the anthracene lattice, like CsI, possesses axes with quite different atomic linear densities. This again could lead to preferential axes of luminescence.
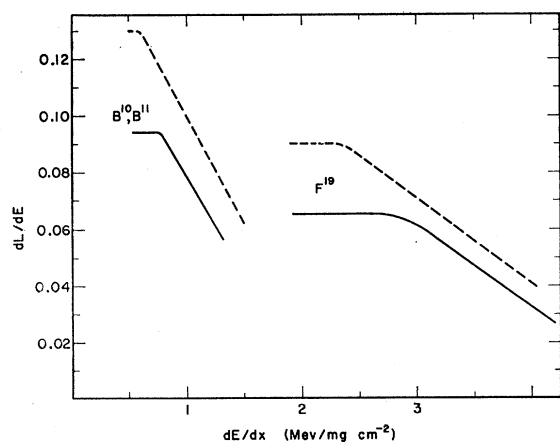

FIG. 4. The differential efficiency of fluorescence for CsI(Tl) as a function of specific energy loss for ions of boron and fluorine. The dashed curves are equivalent relationships for NaI(Tl) crystals.

[5] C. J. Taylor, W. K. Jentschke, M. E. Remley, F. S. Eby, and P. G. Krugen, Phys. Rev. **84**, 1034 (1951).

The curve for the NE 102[6] plastic scintillator is shown in Fig. 3. It exhibited the largest region of linearity of any of the materials examined. This would be in qualitative agreement with the results of Evans and Bellamy[7] for protons. Actually, a slight curvature, commensurate with the small inactivation constant reported, would not be inconsistent with the present data. Even below the velocity region studied, it is apparent that no large saturation effects are necessary to include the origin. The resolution for high energies was typically 3%.

Even a cursory comparison of the three sets of curves would seem to indicate considerable variation among the respective scintillators relative to the light-producing mechanisms involved. Particularly large
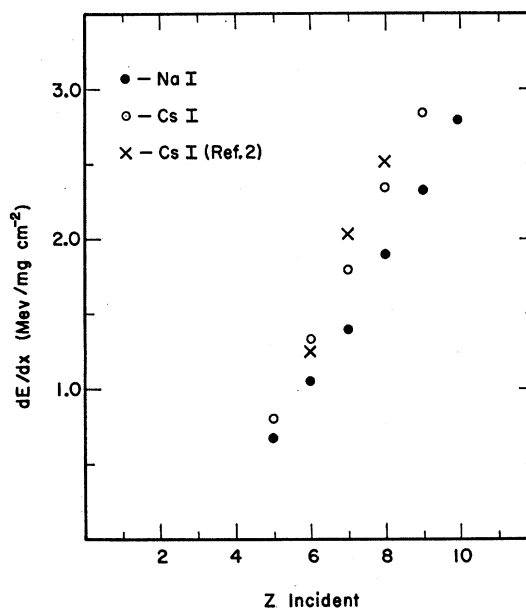

FIG. 5. The value of specific energy loss which appears to be the effective upper limit of linear response as a function of the nuclear charge of the incident ion. Equivalent data for NaI and for CsI as obtained in reference 2 are included for comparison.

differences apparently are involved in the saturation effects usually associated with high specific ionization.

The fluorescent efficiency (dL/dE) for the case of boron and fluorine ions in CsI is displayed in Fig. 4 as a function of the specific energy loss (dE/dx). The values of dE/dx as a function of energy were obtained by extrapolation of the data of Roll and Steigert[8] and of Northcliffe et al.[9] When plotted in this fashion, the regions of linearity (approximately horizontal slope) and saturation are quite apparent. The corresponding

[6] Nuclear Enterprises Ltd.
[7] H. C. Evans and E. H. Bellamy, Proc. Phys. Soc. (London) **74**, 483 (1959).
[8] P. G. Roll and F. E. Steigert, Nuclear Phys. **17**, 54 (1960).
[9] L. C. Northcliffe, Phys. Rev. **120**, 1744 (1960); P. E. Schambra, A. M. Rauth, and L. C. Northcliffe, ibid. **120**, 1758 (1960).

data in NaI are dashed in for comparison. Except for a systematic displacement, the behavior is quite similar in the two. The transition region is rather well defined in each case and occurs consistently at values of dE/dx about 25% higher in the CsI than the NaI. The values of the specific ionization characteristic of this transition region are shown in Fig. 5 for both types of crystal as a function of the incident charge. Since both sets of specific energy-loss curves are constructed from extrapolated values, the precise magnitude of this shift is not as significant as its relative constancy. The values obtained in reference 2 in terms of range in aluminum are included for comparison.

In the saturation region, the slopes for both crystals for the same ion species are roughly parallel. However, this observation is quite sensitive to the systematic scaling errors likely to exist in the constructed specific energy loss curves. One minor difference would be the complete superposition of the two boron curves in CsI.
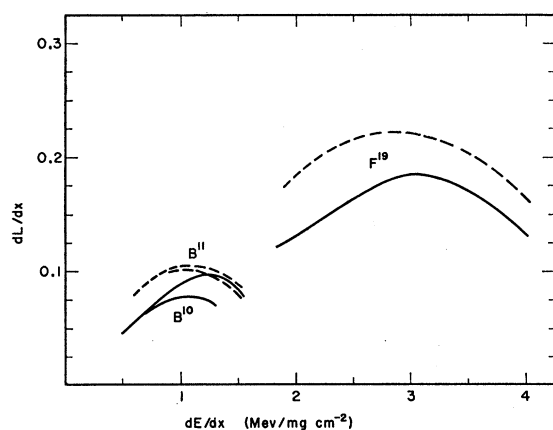

FIG. 6. The specific fluorescence for CsI(Tl) as a function of specific energy loss. The dashed curves are the equivalent relationships for NaI(Tl) crystals.

For the case of NaI, this appeared to be true only in the linear and transition regions. There seemed to be some evidence for a slight divergence at the higher values of dE/dx. For the purposes of the comparisons above, the mean of these two branches was drawn.

An alternative presentation of these same data is as shown in Fig. 6, plotting specific fluorescence (dL/dx) as a function of the specific energy loss. Only the boron and fluorine curves are shown as examples of the behavior in CsI. The corresponding curves in NaI are dashed in for comparison. The general similarity is again apparent. The coefficient of proportionality between dL/dx and dE/dx in the linear (constant slope) region is consistently about 70% of the slopes obtained for NaI. The respective values are displayed as a function of ion species in Fig. 7. It should be noted that an extrapolation of this region does not include the origin. Each of the CsI family of curves would appear to extrapolate to an intercept corresponding to positive
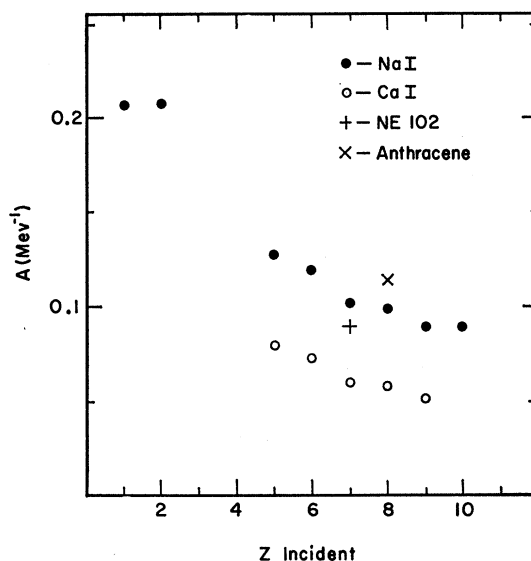

FIG. 7. The coefficient of linearity of the high-energy data as a function of the nuclear charge of the incident particle. The data for NaI is included for comparison.

light output for zero energy loss, similar to the observations for NaI. This is most likely to be accounted for by a small amount of positive curvature in this so called linear region. The behavior of both materials in the saturation region is such as to invalidate Birks'[10] simple assumptions regarding inactivation.

The same relationships are illustrated in Figs. 8 and 9 for the anthracene and NE 102. For these scintillators, only the linear region is reasonably well described. For nitrogen ions in NE 102, the specific luminescence would seem to be strictly proportional to the specific energy loss, with the extrapolated locus even including the origin. From the pulse height data it is apparent,
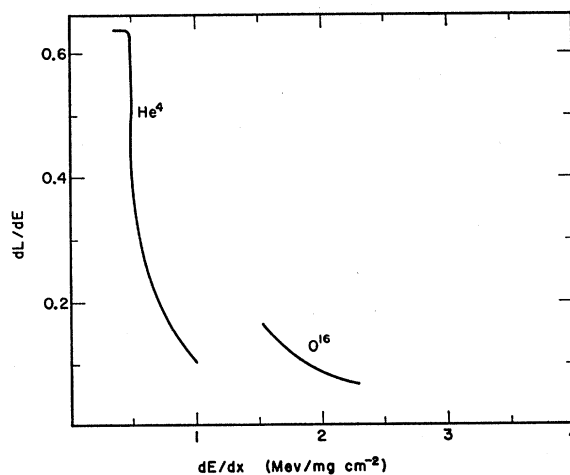

FIG. 8. The differential efficiency of fluorescence for anthracene as a function of specific energy loss for ions of oxygen and helium.

[10] J. B. Birks, *Scintillation Counters* (Pergamon Press, New York, 1953).
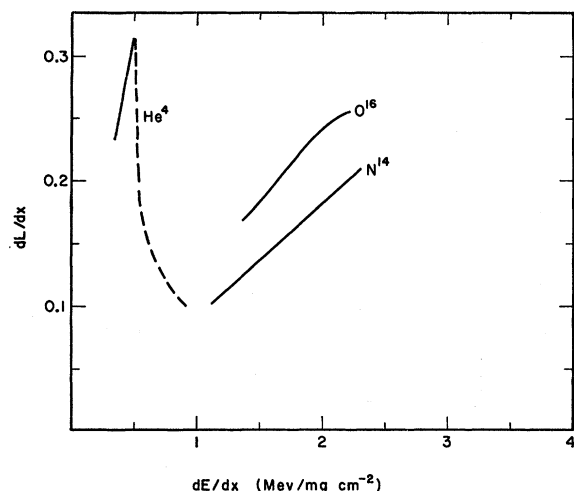
FIG. 9. The specific fluorescence of anthracene and NE 102 as a function of specific energy loss. The nitrogen curve is in NE 102, the oxygen and helium in anthracene. The large dE/dx portion of the helium curve is broken because of the relative uncertainty in measuring the slope of the pertinent portion of the pulse height vs energy curve.

however, that some saturation must be setting in at only slightly higher values of dE/dx. The oxygen in anthracene, in spite of the curvature of the pulse height vs energy plot, shows a reasonably defined linear region. The helium data are somewhat difficult to assess because of the large uncertainty in the values of dL/dE between 4 and 8 Mev per nucleon. The large curvature the pulse height data requires in this region would permit a variety of curves to be drawn, all satisfying the datum points equally well. Accordingly, this portion of Fig. 9 has been dashed in as being questionable. The higher energy data appear to be quite linear, however. Both curves in anthracene extrapolate to about -0.1 mg/cm², roughly the same behavior as previously observed for the alkali halides. These data for the organic crystal are not considered of sufficient accuracy to attach any significance to this approximate coincidence. The respective coefficients of linearity for the heavy ions are compared to those of the alkali halides in Fig. 7.

DISCUSSION

It is apparent that the simple model proposed by Birks to explain the fluorescent response of lightly ionizing particles in organic phosphors is inadequate to understand all features of the present data. The relationship obtained is

$$\frac{dL}{dx} = A\frac{dE}{dx} \bigg/ \left(1 + kB\frac{dE}{dx}\right),$$

where the constant A is to be identified with the light-producing efficiency of the ion-scintillator combination and kB is to be associated with the effective quenching due to local inactivation. Both of the alkali halides demonstrate a falloff in specific fluorescence far stronger than the simple asymptotic saturation expected from this model. However, if the discussion is restricted to the so-called linear regions, the observed behavior is at least compatible with Birks' formulation. The values of the proportionality constant A are then approximately as given in Fig. 7. The corresponding value for alpha particles in anthracene is about 0.5 Mev^{-1} on the basis of the present data. A value of kB of about 0.02 mg cm^{-2}/Mev is sufficient to construct a curve consistent with the datum points in the linear region and also include the origin. This same value of kB will satisfy the anthracene data. While no saturation effects are required to account for the NE 102 results, the experimental points are again not inconsistent with a value of kB as large as 0.01 mg cm^{-2}/Mev, the magnitude observed by Evans and Bellamy[7] for the case of protons.

It would appear that the so-called transition region, corresponding to the knee in Fig. 4, denotes quite well the limit of applicability of this simple picture. For values of dE/dx in excess of this transition value (plotted in Fig. 5) some additional phenomenon would seem to be involved. Ideally, this mechanism would entail a quite high-order loss in sensitivity. Unfortunately, the data in this region is not considered sufficiently accurate to permit parameterization of such higher order terms in the denominator. A more detailed investigation in this low-energy region is obviously called for. One especially strange aspect is that the deviations manifest themselves at increasing values of dE/dx as a function of ion charge rather than some universal limit. This is somewhat inconsistent with the usual concepts of light production requiring the differential fluorescent efficiency (dL/dE) to be a function only of the specific energy loss.

A universalization of the data can be performed in terms of Seitz's[5] generic relationship,

$$L/AZ^2 = h(E/AZ^2),$$

where L, A, Z, and E have the same interpretation as used herein and h denotes some undefined function of the argument. However, considering the inordinately large scaling factors involved (essentially Z^3), such a test would be highly insensitive for most of the present data. Nevertheless, if one considers only the boron data, the appropriate mass ratio of 10/11 accurately describes the two curves shown in Fig. 1.

ACKNOWLEDGMENT